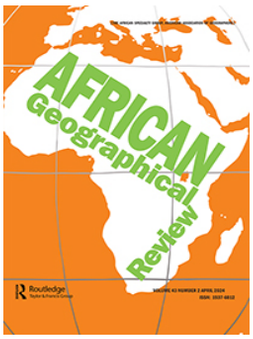

African Geographical Review

ISSN: (Print) (Online) Journal homepage: www.tandfonline.com/journals/rafg20

Geospatial assessment of urban sprawl in Sekondi-Takoradi Metropolis, Ghana from 1991 to 2023

Ernest Biney, Eric Kwabena Forkuo, Michael Poku-Boansi & Yaw Mensah Asare

To cite this article: Ernest Biney, Eric Kwabena Forkuo, Michael Poku-Boansi & Yaw Mensah Asare (26 Mar 2024): Geospatial assessment of urban sprawl in Sekondi-Takoradi Metropolis, Ghana from 1991 to 2023, African Geographical Review, DOI: 10.1080/19376812.2024.2334726

To link to this article: https://doi.org/10.1080/19376812.2024.2334726

AFRICAN GEOGRAPHICAL REVIEW
https://doi.org/10.1080/19376812.2024.2334726

Routledge
Taylor & Francis Group

Geospatial assessment of urban sprawl in Sekondi-Takoradi Metropolis, Ghana from 1991 to 2023

Ernest Biney[a,b], Eric Kwabena Forkuo[a,b], Michael Poku-Boansi[c] and Yaw Mensah Asare[b]

[a]WASCAL Graduate Research Programme on Climate Change and Land Use, Department of Civil Engineering, Kwame Nkrumah University of Science and Technology, Kumasi, Ghana; [b]Department of Geomatic Engineering, Kwame Nkrumah University of Science and Technology, Kumasi, Ghana; [c]Department of Planning, Nkrumah University of Science and Technology, Kumasi, Ghana

ABSTRACT

The upsurge in economic activities and urban dwellers has spurred sprawl-like growth in the Sekondi-Takoradi metropolis. This study used Landsat imageries and Shannon entropy to assess sprawl in the Sekondi-Takoradi metropolis. Analysis of the study revealed an increase in built-up by 63.07 km^2 while Shannon entropy result (which ranged from 2.17 to 2.47), revealed that the metropolis has been sprawling from 1991 to 2023. Hence, causing significant changes in the land cover composition of the metropolis. This study provides valuable insights into the spatial dynamics of the metropolis, which will guide policymakers in addressing the environmental challenges associated with urban expansion.

ARTICLE HISTORY
Received 13 October 2023
Accepted 20 March 2024

KEYWORDS
Urban sprawl; Sekondi-Takoradi; Shannon's entropy; Landsat; Geospatial techniques

1. Introduction

Given how advanced and connected the world has become, the global urban population has increased rapidly from 1 billion in 1960 to 4.4 billion in 2020 (Friedrich, 2021; Tariq et al., 2022). Currently, urban areas accommodate about 55% of the world's population and are estimated to increase to 68% by 2050 (Abass et al., 2022; Rainey et al., 2021). According to Østby (2016), a bulk of the estimated urban population growth will take place in Africa and Asia, and this calls for proper planning to accommodate the growing population. This is because if transformations occurring in urban areas are not adequately managed, they can lead to numerous social, economic, and environmental problems (Aduah & Baffoe, 2013). Globally, industrialization has contributed significantly to transforming rural areas into urban areas, a process known as urbanization. Unfortunately, urbanization adversely results in land cover transformation, primarily marked by an increase in built-up and impervious surfaces (Chettry, 2022). This makes Surya et al. (2021) assert that urbanization is intricately linked to urban sprawl by acting as a catalyst for urban sprawl.

Urban sprawl refers to the dispersion of built-up commonly marked by low-density development, unregulated, and spontaneous growth (Akubia & Bruns, 2019; Feng & Gauthier, 2021). It is characterized by haphazard and random low-density pattern of urban growth, leading to inefficient resource utilization (Kamruzzaman et al., 2018). The sprawl phenomenon, according to the concentric[1] zone theory, occurs when cities expand uncontrollably by extending their concentric land use zones outwards from Central Business District (CBD). Research by Getu and Bhat (2021), and Shao et al. (2021) highlight that urban sprawl is primarily exacerbated by rapid population and socio-economic development, and its occurrence in both developed and developing countries has made it an issue of global concern. In developed

CONTACT Ernest Biney ernest_biney@yahoo.com

This article has been corrected with minor changes. These changes do not impact the academic content of the article.

nations, urban sprawl becomes worse after reaching saturation levels of urbanization. However, most developing countries, at the beginning of urbanization are predisposed to sprawl at an exacerbated scale due to high population growth and densities, characterized by inadequate basic amenities and infrastructure, unlike the developed countries where the saturated level of urbanization is fueled by industrialization, technological support, and a prosperous economy (Krishnaveni & Anil, 2022).

In Ghana, urban sprawl is characterized by the extensive and unrestricted outward growth of urban areas at the expense of other land cover types, in a manner that does not follow the spatial plan of the city (Frimpong et al., 2022; Nyamekye et al., 2020). A report by the Sekondi-Takoradi Metropolitan Assembly (STMA) asserts that the metropolis is experiencing a surge in its socio-economic activities (Mensah et al., 2019). This increase became phenomenal in 2007 after the discovery of oil in commercial quantities and has been a point of attraction for many individuals resulting in an excessive rise in the real estate sector and human population (Fiave, 2017). For instance, before the oil discovery in 2000, the metropolis had a population of about 360,000. However, after commercial oil exploitation started in 2010, the population stood at about 560,000 (Fiave, 2017). The increase in the urban population during that time brought a corresponding increase in the demand for land for various purposes. As a result, pressure was put on land availability and this brought drastic changes to the land use pattern and land cover characteristics within the metropolis (Stemn & Agyapong, 2014). In this regard, between 2010 and 2013, the spatial development planning unit of Sekondi-Takoradi Metropolis stressed that the changing physical landscape is due to pressures on land for various development projects (Alqattan et al., 2019; Danso & Addo, 2018; Mensah et al., 2019; Vinh & Nguyen, 2019). Unfortunately, these modifications have an adverse impact on the city's sustainability, and this goes contrary to the global development agenda of cities achieving sustainable communities by 2030, specifically, against the sustainable development goal (SDG) 11 of 'making cities inclusive, safe, resilient and sustainable' (United Nations, 2015). Currently, research work by Biney and Boakye (2021) and Mensah et al. (2019) reveals that the metropolis is experiencing an excessive increase in the built-up, which also signifies an increase in impervious surfaces in the metropolis. This escalating rate of impervious surfaces is not encouraged in sustainable cities due to their poor infiltration capacity, high run-off, and low albedo effect. Hence, creating problems like flooding and urban heat islands. In this light, Aduah and Baffoe (2013) assert that if changes in urban areas are not properly handled, they can result in many social, economic, and environmental tragedies. Fortunately, since the establishment of the Takoradi harbor, airport, railways, market circle, and industries, Sekondi-Takoradi has been a business hub for major local, national, and international organizations. Therefore, any disaster in Sekondi-Takoradi will have a roll-over effect on the national economy and to some extent the global economy (Abdul-Kareem et al., 2021). It is against this background that this study aims to assess urban sprawl in the Sekondi-Takoradi metropolis.

Geographic Information Systems (GIS) and Remote Sensing (RS) have been effectively used to monitor land cover change and assess urban sprawl compared to conventional survey techniques (Shao et al., 2021). This viewpoint is validated by Hasan et al. (2023) and Rana and Sarkar (2021) as their studies showed that employing GIS and remote sensing are cost-effective and time-efficient methods to quantitatively analyze urban sprawl. Shikary and Rudra (2020) highlight that effective assessment of urban sprawl requires using efficient techniques to comprehend the present state and pattern of urban expansion. This, according to Sumari et al. (2020), can be achieved through the combined application of geospatial techniques and spatial metrics such as Shannon's entropy. Shannon's entropy quantifies the degree of compactness or dispersion of a geospatial element (Deribew, 2020; Ibrahim et al., 2019). Its computation has aided in comprehending the trend and pattern of urban growth occurrence across the urban space (Shikary & Rudra, 2020) and this makes it a valuable method for quantifying and monitoring urban sprawl. Therefore, using remotely sensed data, GIS, and Shannon's entropy model, the objective of the study is to examine both past and current land use patterns and quantify the trend of urban growth of the Sekondi-Takoradi metropolis. The approach employed in this study can be used to evaluate urban growth in other

cities in Ghana or other developing nations with comparable conditions. Also, knowledge from this study will enable city planners and policymakers to gain a comprehensive understanding of the multifaceted aspects and spatio-temporal dynamics of urban sprawl, which will enable them to allocate resources efficiently and implement effective infrastructure management strategies accordingly. This paper is broadly sectioned as follows: 1. General overview of urban growth; 2. Description of materials and methods; 3. Results and discussions; 4. Conclusion of the study.

2. Materials and methods

The materials and methods used in the study are detailed in the subsequent subsections.

2.1. Study area

Sekondi-Takoradi Metropolis (Figure 1) is situated in the Western region of Ghana and lies between Latitude 4° 52'30'N and 5° 04' 00' N, as well as Longitudes 1° 37'00'W and 1° 52' 30' W. The metropolis has an area of approximately 191.7 km^2. It shares borders with Wassa East District to the North, the Gulf of Guinea to the South, Shama District to the East, and Ahanta West District to the West. By 2010, the metropolis had a population of 559,548 (PHC, 2010). However, by 2021, the population increased to 734,645 (Dadzie-Paintsil & Mensah, 2022). This proves that a large number of the people living within the metropolis live in urban areas. Sekondi-Takoradi was chosen because it serves as the hub for economic and political activities for the Western Region and the nation at large. However, the extent to which this study area's urban growth has been studied in terms of its pattern, magnitude, rate, and spatiotemporal characteristics, as well as its effects on the other LULC categories remains insufficient, especially in an era where its rate of urbanization makes it the third urbanized metropolis in Ghana.

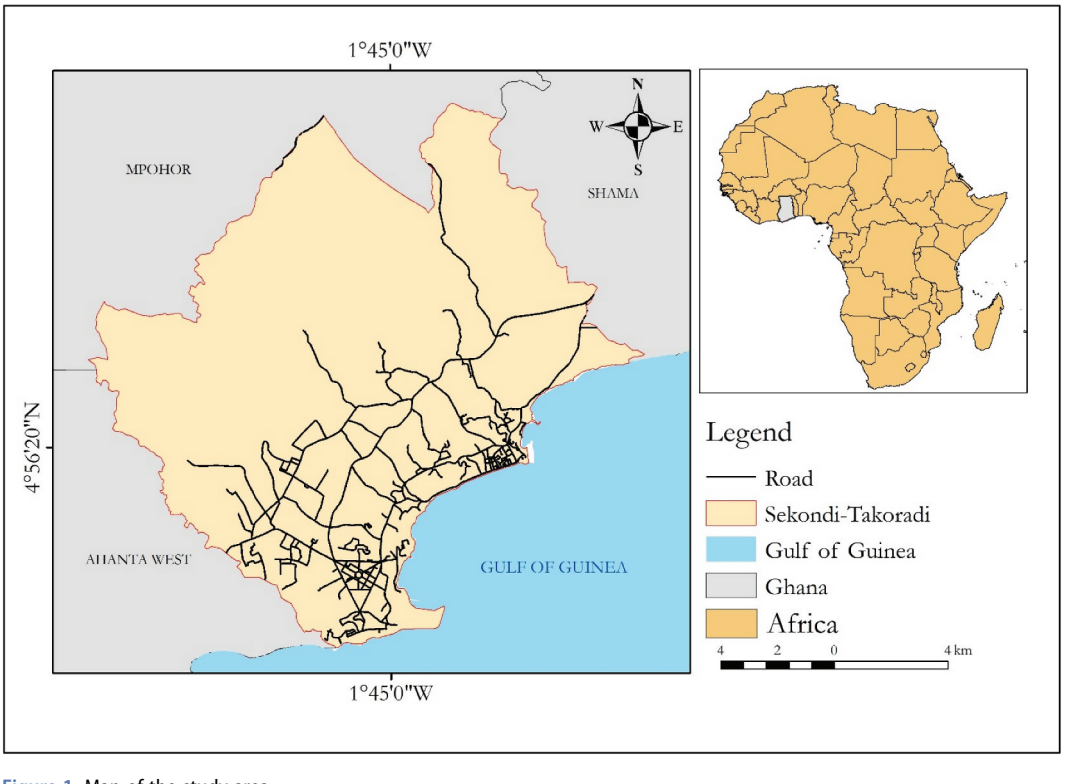

Figure 1. Map of the study area.

2.2. Datasets used and software

Table 1 displays the data used for the study. The irregularity in the image intervals stemmed from insufficient data with less than 10% cloud cover. The pre-processing and processing of the Landsat images employed various software such as ArcGIS Pro, Google Earth Engine, and QGIS. Specifically, the QGIS and Google Earth Engine were used for pre-processing, classification, accuracy assessment, and creating transitional probability. ArcGIS Pro was utilized to generate all classified maps and output maps.

Table 1. Dataset used for the study.

Satellite Data	Resolution	Date Acquired	Source	No. of bands
Landsat TM	30m	01/01/1991	USGS	7
Landsat ETM+	30m	01/02/2009	USGS	8
Landsat ETM+	30m	01/01/2016	USGS	8
Landsat OLI/TRIS	30m	01/01/2023	USGS	11
Reference data				
Google Earth images		1991, 2009, 2016 and 2023	Google earth explorer	

2.3. Methods

According to Getu and Bhat (2021), detecting significant changes in multi-temporal images involves a series of activities and complex processes to obtain precise and accurate information. Therefore, the following processes as outlined in Figure 2 and elaborated in the subsequent sub-sections were carried out for this study.

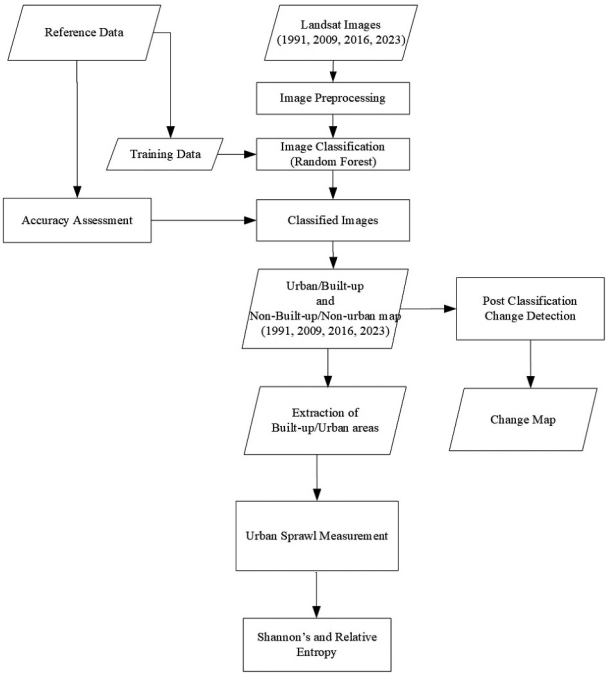

Figure 2. Methodological flowchart.

2.3.1. Image pre-processing

Before image classification can be done efficiently, a satellite image needs to be preprocessed to correct any error encountered during its imaging (Gašparović, 2020). Geometric and Radiometric corrections and image band staking were the pre-processing types conducted in this study. The obtained Landsat images were geometrically corrected from the source. However, to maintain consistency in both the size and positioning of the obtained images, image-to-image registration was conducted in QGIS. The 2023 Landsat image served as the base image for this process, followed by reprojection to UTM '84 zone 30N (Abudu et al., 2019). According to Anwar et al. (2022), errors that affect the quality of digital numbers of satellite images can be improved by radiometric correction. The Semi-Automatic Classification (SCP) plugin in QGIS was used to radiometrically correct the images and then band stacked to form composite bands which could be visualized in different color combinations. According to Abass et al. (2018), False Colour Composite (FCC) produces distinct spectral signatures for easy identification of land color classes. Therefore, this study used FCC to identify the land cover classes.

2.3.2. Image classification

Image classification is the process of obtaining information by grouping all pixels in an image to have a set of classes (Saha et al., 2021). The supervised classification technique was used in this study to categorize the images into their appropriate classes after training samples, and signature classes had been established. Based on the objectives of the study and employing an acceptable categorization method, the study area was classified into non-built-up and built-up (Table 2).

Like much research, this study employed a supervised technique for classifying images. The supervised classification is based on the concept of using samples with known identities to categorize pixels with unknown identities (Anwar et al., 2022). Specifically, Random Forest (RF) supervised classification method was used to classify the images. This supervised classification technique was chosen because it generates higher classification accuracy even when applied to data with higher noise levels compared to other classifiers like Support Vector Machine (SVM), Classification, and Regression Tress (Hidalgo-García & Arco-Díaz, 2022; Xiang et al., 2022). This has been proven in the works of Fernández-Delgado (2014), who evaluated 179 relevant classifiers from 17 families using 121 datasets and found random forest to be the best classifier. Additionally, RF can manage missing values, categorical and unbalanced data- a capacity which is not present in SVM (Haas, 2013).

Table 2. Description of the land cover classes.

CLASS	Description
Non-Built-up	Waterbodies and vegetative areas.
Built-up	These include paved areas, impervious surfaces, roads, bare lands, residential areas, areas covered by man-made structures, and commercial areas.

2.3.3. Accuracy assessment

Land use land cover classification with inaccuracies affects the genuineness of the analysis (Mohammadian et al., 2017), therefore, to prevent such a situation, an accuracy assessment needs to be performed. In this study, the confusion matrix was used to assess the performance of the classified images (Foody, 2020). Various measures such as overall accuracy (*OA*), kappa coefficient (*K*), user's (*UA*), and producer's accuracy (*PA*) that are directly used as indicators of either overall accuracy assessment or individual class assessment were computed from the confusion matrix. The accuracy assessment parameters used in the classification accuracy can be expressed mathematically in the following Equations (1-4) (Shamsudeen et al., 2022).

$$UA = \frac{Number\ of\ correctly\ classified\ pixels\ in\ each\ category}{Total\ number\ of\ classified\ pixels\ in\ that\ category} \times 100 \tag{1}$$

$$\mathrm{PA} = \frac{\text{Number of correctly classified pixels in eacg category}}{\text{Total number of classified pixels in that category}} \times 100 \tag{2}$$

$$OA = \frac{Total\ number\ of\ correctly\ classified\ pixels}{Total\ number\ of\ reference\ pixels\} \times 100} \tag{3}$$

$$K = \frac{\boldsymbol{N}\sum_{i=1}^{r}\boldsymbol{x_{ii}} - \sum_{i=1}^{r}(\boldsymbol{x_{i+}} \times \boldsymbol{x_{+i}})}{\boldsymbol{N}^2 - \sum_{i=1}^{r}(\boldsymbol{x_{i+}} \times \boldsymbol{x_{+i}})} \tag{4}$$

Where N is the total number of samples in the matrix, r corresponds to the number of the rows in the matrix, x_{ii} is the number in row I and column i, x_{+i} is the total for row i, and x_{i+} is the total for column i

2.3.4. Change detection

In this study, post-classification change detection was used because it gives detailed information about changes that take place from one class to another. These changes make it possible to create a change matrix that aids in tracking pixel changes over two time periods to determine the trade-offs between the classes (Alijani et al., 2020; Asare et al., 2023). Also, the annual rate of change and percentage annual rate of change was computed using Equation (5) and (6), respectively, as part of the post-classification change detection (Deribew, 2020).

$$A_r = \left(\frac{A_2 - A_1}{T}\right) \tag{5}$$

Where A_r is the annual rate of change, A_2 is the current area of land use land cover type in km^2 and A_1 is the initial area of land cover type in km^2, and T= time interval between the initial year (A_1) and the current year (A_2).

$$C = \left[\left(\frac{F - I}{I}\right) * \left(\frac{1}{T}\right)\right] * 100 \tag{6}$$

Where 'C' is the percentage annual rate of change, "F "is the final year, 'I' is the initial year, and 'T' is the time period (interval) between the final year and the initial year.

2.3.5. Transition of land use land cover changes

This study employed a cross-tabulation matrix to ascertain changes within and across all classified cover classes. The output of a cross-tabulation matrix, according to Abdullahi and

Pradhan (2010), can be in four types: 1. cross-classification image, 2. full cross-tabulation table, 3. both cross-classification image and cross-tabulation table, and 4. image similarity data only. Output type 3 was chosen for this study. Four cross-tabulation tables were produced for this study (Table 5). In the tabulation table, the diagonal elements signify unchanged classes while the off-diagonal elements denote classes that have changed. Also, the horizontal and vertical elements, respectively, represent classes in the later (second) and earlier (first) periods. The sum of each row and column in the table indicates either a gain or loss in the various classes.

2.3.6. Measurement of urban sprawl

Urban sprawl from the period of 1991 to 2023 was determined using Shannon and relative entropy. Before the measurement of sprawl, built-up was extracted from the classified images. The center point of the metropolis, which is the Central Business District (CBD), was divided into several concentric zones (Figure 6). Concentric buffers were chosen for this study because they properly capture the shape of the study area. The study area was partitioned into 17 concentric buffer zones at an interval of 1 km between each zone (Manesha et al., 2021). The 1 km interval distance was chosen because it captures all of the built-ups within a buffer zone, provides clear information on the distribution of small growth, and is not subject to potential modifiable area unit problem (MAUP) (Deribew, 2020; García-Álvarez et al., 2022). The zonal statistics tool in QGIS was used to calculate built-up quantity in each zone and the overall built-up area. The output of the zonal statistics was transferred to Microsoft Excel for further computation and analysis using the Shannon and relative entropy formulas. These spatial metrics are commonly used to quantify the degree of built-up area concentration or dispersion (Frimpong et al., 2022; Getu & Bhat, 2021). The Shannon entropy (E_n) was computed using Equation (7) (Deribew, 2020; Steurer & Bayr, 2020):

$$E_n = \sum_{i=1}^{n} P_i * \ln\left(\frac{1}{P_i}\right) \tag{7}$$

From Equation (7), *Pi* which is the density of land development, expressed in Equation (8) is defined as the quantity of built-up area in each zone (X_i) divided by the total number of built-up of the total zones. n represents the total number of zones.

$$P_i = \frac{x_i}{\sum_i^n x_i} \tag{8}$$

The values of E_n vary from 0 to Ln (n). A value closer to 0 indicates a concentrated distribution of the spatial variable, while a value closer to Ln (n) suggests a dispersed distribution (Al-Hinai & Abdalla, 2021; Alqadhi et al., 2021). Nonetheless, using the relative entropy (H'_n) to normalize the entropy values to 0 and 1 is preferable (Manesha et al., 2021; Steurer & Bayr, 2020). According to Abudu et al. (2019), a city is experiencing sprawling if the entropy value exceeds the threshold of 0.5 for relative entropy and half of the log of the number of zones for Shannon entropy.

$$H'_n = \frac{\left(\sum_{i=1}^{n} P_i * \ln\left(\frac{1}{P_i}\right)\right)}{\ln(n)} \tag{9}$$

The magnitude of change in entropy was also computed by determining the difference between the entropy of initial year $E_n(t1)$ and the current year $E_n(t2)$. Using Equation (10), the magnitude of urban sprawl was computed (Chong, 2017; Getu & Bhat, 2021)

$$\Delta E_n = E_n(t2) - E_n(t1) \tag{10}$$

3. Results and discussion

The findings of this study are comprehensively presented and discussed across the following sub-themes: classified land use land cover, accuracy assessment, transition matrix, urban expansion analysis, and urban sprawl analysis.

3.1. Classified land use land cover

By visual interpretation, the metropolis showed signs of growth from the central business district, along the coastal corridor, and along the main roads that link the metropolis to other cities. The Western and the Southern-Western part of the study clearly have experienced significant growth (Figure 3). This type of urban growth can be seen in some coastal cities in Ghana such as Cape Coast and Accra (Service, 2021) and it can be explained by the fact that a city's main road network, the presence of seaport and airport have a significant impact on its population density (Hackman et al., 2020) which is the case of the western and southern part of the metropolis. A statistical analysis of Figure 3 is presented in Table 3.

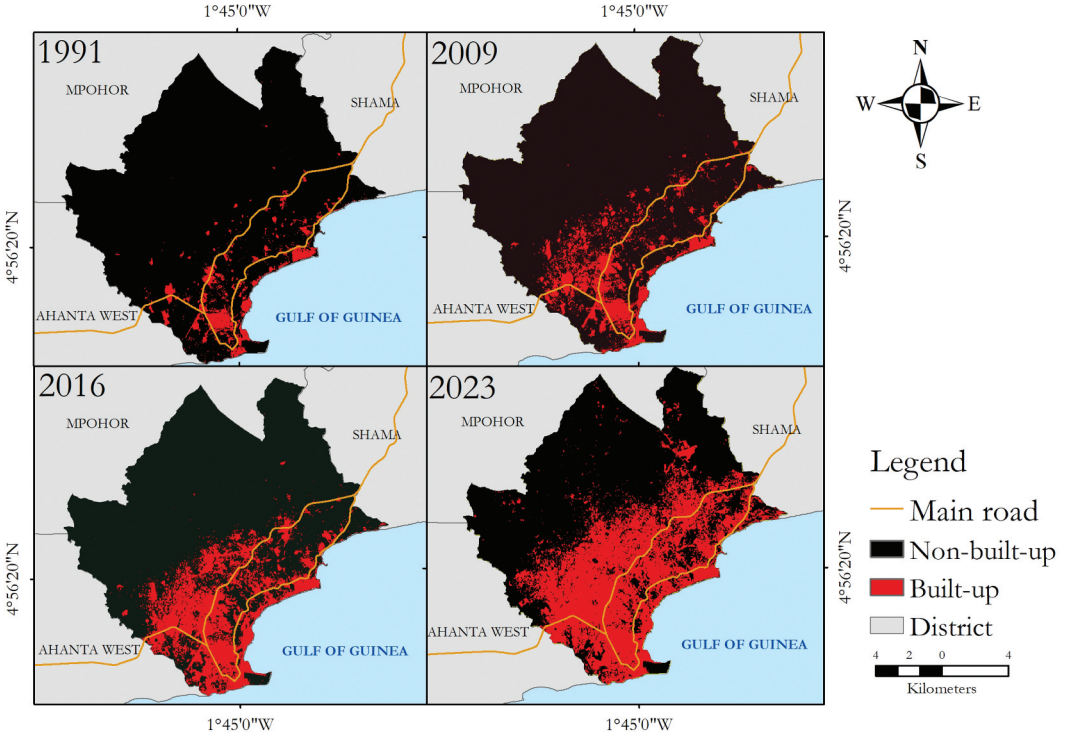

Figure 3. Map of built-up and non-built-up.

Table 3. Statistics of classes from 1991 to 2023.

Year	Total Area (km^2)	Non-Built-up (km^2)	Non-Built-up (%)	Built-up (km^2)	Built-up (%)	Change in Built-up (km^2)	Change in Built-up (%)
1991	191.66	181.10	94.49	10.56	5.51	-	-
2009	191.66	169.53	88.45	22.13	11.55	11.57	6.04
2016	191.66	152.68	79.66	38.98	20.33	16.85	8.79
2023	191.66	118.03	61.58	73.63	38.42	34.65	18.08

From Table 3, built-up increased significantly throughout the study period at the expense of a drastic decline in the area of non-built-up. This suggests a significant urban expansion in the study area and reflects a shift in land use from natural or undeveloped spaces to developed or urbanized areas. The increase in built-up, as a consequence of the persistent decrease in non-built-up, could be attributed to the increasing demand for land for constructional purposes influenced by population growth and an increase in economic activities that are largely linked to the oil discovery (Fiave, 2017; Mensah et al., 2019). This correlation is highlighted in the 2021 Population and Housing Census of Ghana (Service, 2021) and is further substantiated by Dadzie-Paintsil and Mensah (2022). Predating the oil discovery, 359,363 people lived in the metropolis. Following the oil discovery, the population grew to 559, 548 in 2010 (Service, 2014). The population surge coincided with an increase in the demand for land for residential, commercial, and industrial purposes, resulting in the transformation of diverse land cover into built-up areas (Fiave, 2017). Figure 4 supports the claim of Fiave (2017) as population data from the United Nations World Population Prospect (2023) concurrently correspond to the increase in built-up over the study period.

According to Mensah et al. (2019), the demand for housing, particularly in 2011, prompted immediate action from real estate developers, resulting in the initiation of housing projects such as the Takoradi Oil Village and King City to accommodate the expanding population. Additionally, many establishments within the hospitality sector underwent renovations and expanded their facilities to take in more guests while new establishments sprang up to cater to the needs and

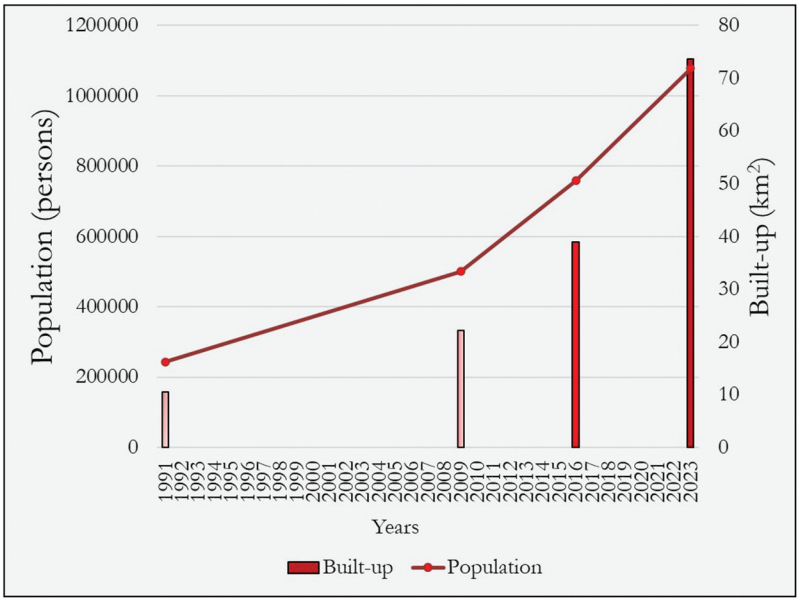

Figure 4. The pattern of population growth and expansion of built-up areas.

address the accommodation requirements of high-income expatriates from the oil industry who moved to the metropolis (Biney & Boakye, 2021). Furthermore, from 2011 to 2016, the construction of the N1 road and the dualization of single roads to enhance transportation infrastructure transformed several hectares of diverse land cover into impermeable surfaces (Mensah et al., 2019). Currently, the construction of the Kwame Nkrumah interchange, which began in 2020 as well as the expansion of the road from the Paa Grant roundabout to Sekondi, has claimed several vegetative land and wetland lands (Annim, 2023). Lastly, during the Takoradi Port development in 2016, approximately 530 km^2 of cultivated land was transformed into impermeable surfaces (GPHA, 2016). These developments have played a crucial role in the expanding built-up areas in the metropolis.

Studies by Aduah and Baffoe (2013), revealed that waterways, which are a component of non-built-up are being converted into built-up. These waterways are frequently filled with sand and prepped for building and other construction activities. A notable case is the Anankori River, where boulders have been used to fill several of its tributaries to allow tipper vehicles to transport sand and stones from the river (Biney & Boakye, 2021). Currently, the condition of these waterways and waterbodies compared to their state in the 1990s indicates a significant rate of encroachment and conversion into built-up areas. Hence, depriving the metropolis of the benefits that come with water conversation (Danso & Addo, 2018). This aligns with the claims of Mohammadian et al. (2017) and Wangyel et al. (2021) that the growth of built-up areas can negatively affect areas covered by water if they are not efficiently monitored. Furthermore, the decline in the non-built-up area is consistent with the notion that vegetation mostly suffers losses when a city is expanding (Appiah, 2016; Biney et al., 2022; Daata et al., 2021). The Service (2014) reports that since 1991, there has been a notable migration wave into the Sekondi-Takoradi metropolitan. Due to the pressure that the population surge has placed on the existing green spaces, private estate developers and individuals have begun to convert lands both within and outside of the urban perimeter.

The significant changes in the cover classes presented in Table 3 occurred at an increasing annual rate for built-up and a decreasing annual rate for non-built-up (Figure 5). Throughout the study period, built-up increased while non-built-up declined by 1.97 km^2 annually.

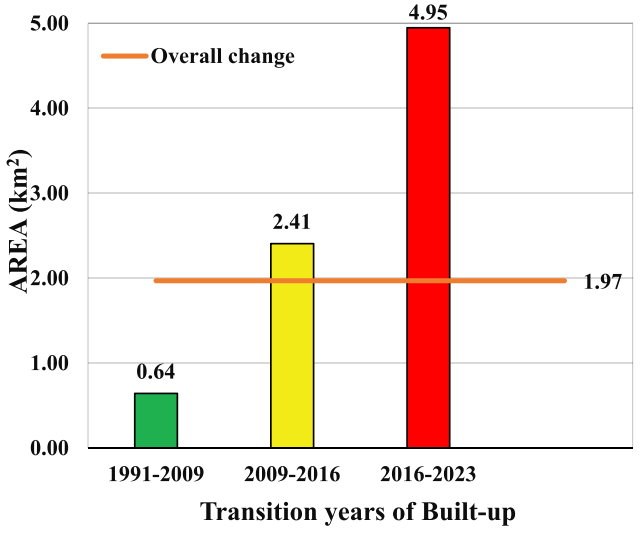

Figure 5. Annual rate of change from 1991 and 2023.

3.2. Accuracy assessment of LULC classification

Obeng et al. (2023) assert that image classification with kappa values higher than 0.7 and an overall accuracy of 85% is indicative of quality classification. The accuracy values presented in Table 4 exceeded the minimum accuracy standard proposed by Obeng et al. (2023). Therefore, the classification results were used for further computation and analysis specifically, change detection analysis.

Table 4. Classification accuracy.

	Producer's Accuracy		User's Accuracy			
Year	Non-built-up	Built-up	Non-Built-up	Built-up	Overall Accuracy (%)	Kappa Coefficient
1991	92.69	90.68	90.89	94.60	*92.69*	*0.85*
2009	98.31	90.76	86.63	98.88	*93.62*	*0.87*
2016	94.95	93.56	92.25	95.83	*94.18*	*0.88*
2023	97.58	93.22	93.25	97.57	***95.36***	***0.91***

3.3. Change detection analysis

A change detection matrix table (Table 5) and transition maps (Figure 6) were used to understand the transformation that occurred during the study period.

Table 5. Transition area matrices of LULC from 1991 to 2023.

		2009		
	LULC Class	Non-built-up (km^2)	Built-up (km^2)	Total of 1991
1991	Non-built-up	**168.07**	13.03	**181.10**
	Built-up	1.46	**9.10**	**10.56**
	Total of 2009	**169.53**	**22.13**	**191.66**
	Net change	*−11.57*	*11.57*	
	Total unchanged	*177.17 (92.44%)*		
2016				
	LULC Class	Non-built-up (**km^2**)	**Built-up (km^2)**	**Total of 2009**
2009	Non-built-up	**150.85**	18.68	**169.53**
	Built-up	1.83	**20.30**	**22.13**
	Total of 2016	**152.68**	**38.98**	
	Net change	*−16.85*	*16.85*	
	Total unchanged	*171.15 (89.30%)*		
2023				
	LULC Class	Non-built-up (**km^2**)	**Built-up (km^2)**	**Total of 2016**
2016	Non-built-up	**117.10**	L35.58	**152.68**
	Built-up	0.93	**38.05**	**38.98**
	Total of 2023	**118.03**	**73.63**	
	Net change	*−34.65*	*34.65*	
	Total unchanged	*155.15 (80.98%)*		
2023				
	LULC Class	Non-built-up (**km^2**)	**Built-up (km^2)**	**Total of 1991**
1991	Non-built-up	**117.77**	63.33	**181.10**
	Built-up	0.26	**10.30**	**10.56**
	Total of 2023	**118.03**	**73.63**	
	Net change	*−63.07*	*63.07*	
	Total unchanged	*128.07(66.83%)*		

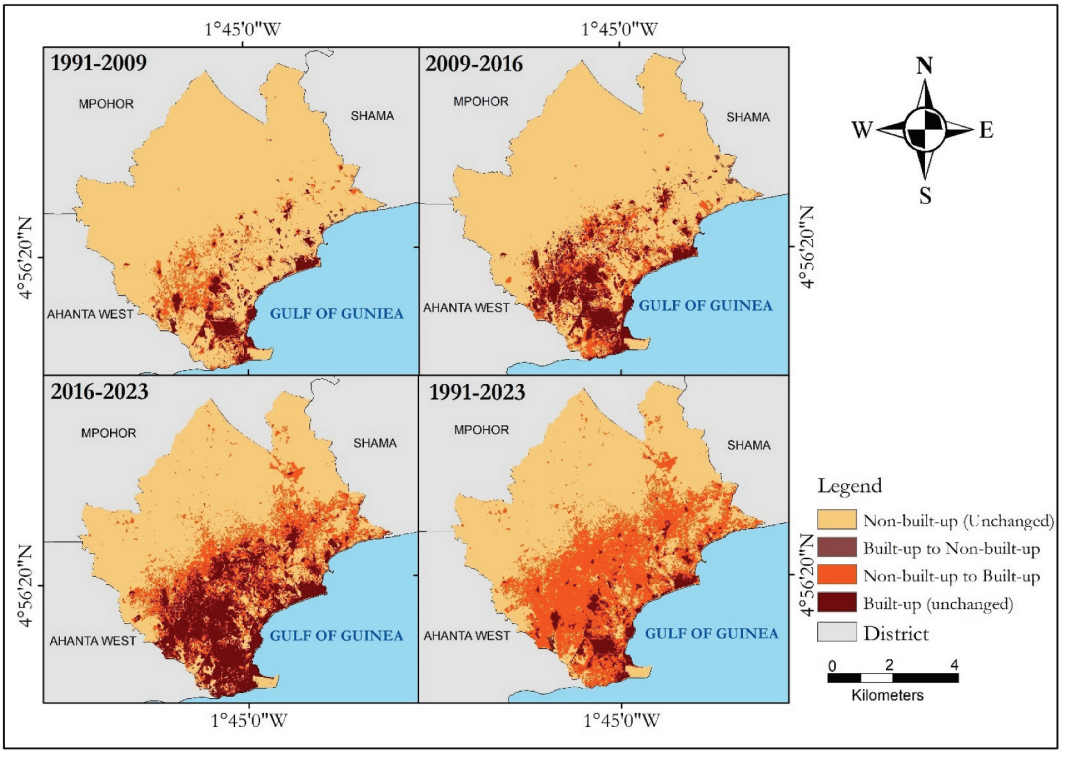

Figure 6. Transition maps.

Between 1991 and 2009, it can be observed from Table 5 that 168.07 km^2 of non-built-up and 9.10 km^2 of built-up did not change. These unchanged classes covered a total of 177.17 km^2 (92.44%) while the classes that changed covered a total of 14.49 km^2 (7.56%). The increasing change in non-built-up to built-up is due to the dint of increasing anthropogenic activities that occurred through the infrastructural development. This is proven by the substantial decrease in non-built-up. From 2009 to 2016, the total land cover classes that remained unchanged covered an area of 171.15 km^2 (89.30%), and the total land cover types that changed occupied an area of 20.51 km^2 (10.70%). The unchanged area, in contrast to the transitional phase between 1991 and 2009 experienced a reduction of 6.02 km^2. Between 2016 and 2023, the total number of land use classes that remained unchanged was 155.15 km^2 (80.98%) while the total area of classes that changed was 36.51 km^2 (19.02%). The unchanged area, when compared to the transition period of 2009 and 2016, decreased by 16 km^2. Generally, between 1991 and 2023, the total number of land use classes that remained unchanged was 128.07 km^2 (66.82%) while the total area of classes that changed was 63.59 km^2 (33.18%). Remarkably, built-up increased by 63.08 km^2 and this was at a considerable decline in non-built-up by 63.07 km^2. This analysis underscores the increasing trend of converting non-built-up land into built-up areas, highlighting a visible degradation in non-built-up areas, especially its components.

3.4. Urban sprawl analysis

The analysis of urban sprawl was carried out by first partitioning the built-up areas into concentric zones (Figure 7), and second by applying the Shannon and relative entropy (Table 6).

3.4.1. Built-up density of concentric ring buffer

The built-up images were fragmented into 17 concentric zones at an interval of 1 km between the zones, starting from the city center (Figure 7). This division was done to assess sprawl for the various years and to aid in defining the direction of urban land growth (Verma et al., 2021).

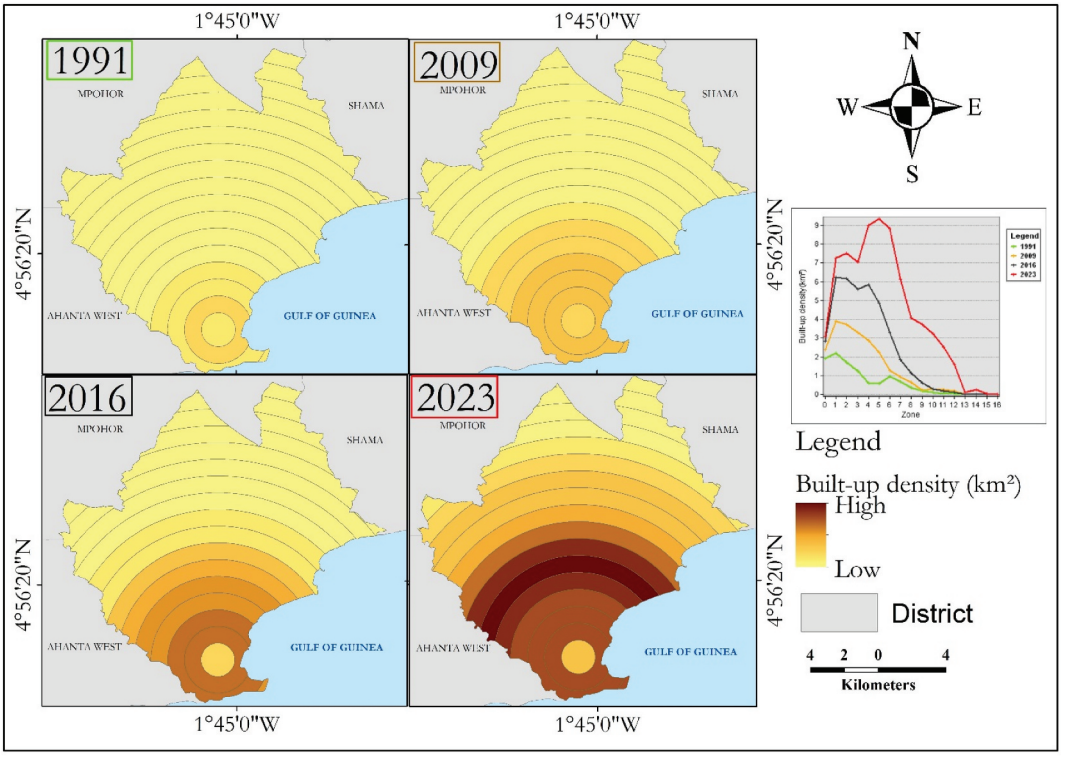

Figure 7. Built-up density map.

It can be seen in Figure 7 that there was an irregular increase and decrease in the built-up density in all the zones for the various years. This could be explained by the existence of various pull factors during the time of urban growth (Agenda, 2013; Doe et al., 2022). However, comparing the values in each zone to the zones of the subsequent years, an increasing trend was observed among the various years which signifies an increase in urban development. From the city center to about the 7th zone, built-up density was relatively high for all years but mostly decreased as it extended further from the 7th Zone. This means built-up has expanded into the fringes of the metropolis and as pointed out by Krishnaveni and Anil (2022) and Mensah et al. (2019), it will bring several adverse implications like the loss of vegetative cover and green spaces, increased infrastructure costs (Rainey et al., 2021), increased carbon emissions (Feng & Gauthier, 2021; Frimpong et al., 2022), increased traffic congestion (Mukherjee & Singh, 2020), increase energy consumption (Hackman et al., 2020), and decrease social cohesion (Mohammadian et al., 2017).

3.4.2. Quantification of urban sprawl using relative and Shannon's entropy

According to Cengiz et al. (2022), the growth of urban areas predominantly relies on the transformation of various Land Use Land Cover (LULC) categories. Therefore, it is crucial to evaluate the

pattern of LULC to comprehend the dynamics within the land cover classes that contribute to urban growth. One effective method for conducting this evaluation is through the application of spatial metrics such as the Shannon and relative entropy. From Table 6, the entropy values showed an irregular pattern despite the relatively high entropy values for the various years. By examining the Shannon and relative entropy values of the various timesteps against their thresholds, it was evident that all the years had values greater than the thresholds which according to Krishnaveni and Anil (2022), denotes dispersion taking place in all the years. The lowest entropy occurred in 1991 while the highest entropy was recorded in 2023 (Table 6). This finding reveals that in 2023, the city exhibited a greater degree of sprawl than in other years. The reason for the significant dispersion in 2023 could be explained by the increasing infrastructural construction at the fringes of the city (Mensah et al., 2019; Service, 2021).

Additionally, although the metropolis has been sprawling, the rate of sprawl is not uniform. The change in entropy shows that the dispersion was highest between 2016 and 2023 and lowest between 1991 and 2009 (Figure 8). Unfortunately, the significant disparities in the entropy values over 32

Table 6. Shannon and relative entropy.

Year	Built-up (km^2)	Shannon entropy	Relative entropy
1991	10.56	2.17	0.76
2009	22.12	2.27	0.80
2016	38.98	2.20	0.77
2023	73.63	2.47	0.87
Maximum entropy	-	2.83	1
Threshold	-	1.42	0.5

years will make it difficult to achieve goal 11 of the sustainable development goals (SDGs) and also threaten the existence of other land cover classes in the metropolis (Dijkstra et al., 2022). It is recommended that the metropolis should implement stringent land use regulations and prioritize sustainable urban development practices. This will align the metropolis with the sustainable development goal 11 of making human settlements safe, sustainable, and resilient (Larbi, 2023).

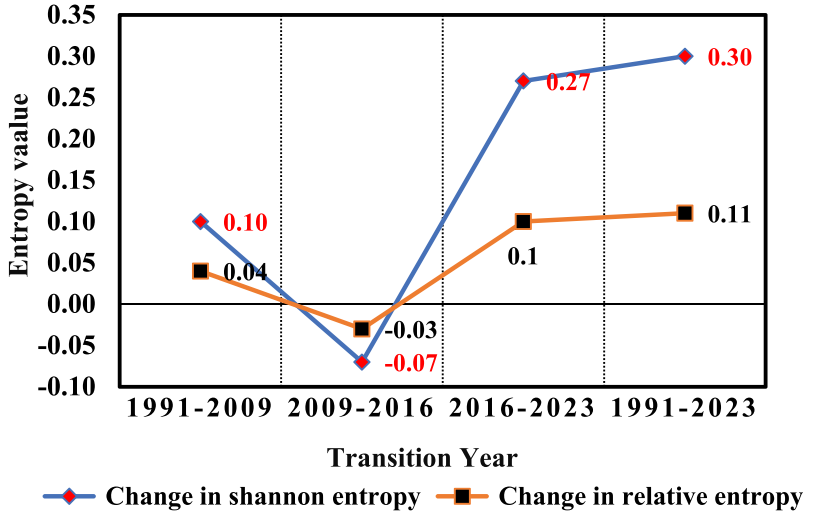

Figure 8. Change in entropy.

3.5. Conclusion

Understanding the configuration of urban sprawl is vital in creating an inclusive, safe, resilient, and sustainable urban environment. This study employed Landsat images and spatial metrics to assess urban sprawl in Sekondi-Takoradi metropolis from 1991 to 2023. Through the use of the supervised random forest classification algorithm, the images were classified into two classes which were aimed at examining the growth pattern of the metropolis. Results from the 32-year period revealed that built-up increased by 63.07 km^2. In addition, the study showed that the metropolis has expanded its sphere of influence greatly to the south and south-western boundary through the annexation of adjacent communities. Moreover, using Shannon's and relative entropy to measure sprawl in the metropolis, it was observed that sprawling in the study area started as early as 1991. However, the study was limited by the following challenges. First, there were discrepancies in the acquisition dates of the satellite images due to issues of cloud cover. A more robust analysis and conclusion could be made if the images had the same time interval. Second, due to the spatial resolution of the Landsat images, changes that occur on small scales cannot be effectively identified. These challenges should be taken into account for future studies. Despite these challenges, the findings remain valuable for city authorities and urban planners. They can leverage on these findings to tackle land-use regulation issues and to create effective strategies and policies that optimize the distribution of resources and infrastructure. Also, the methodology employed in this study could be adapted to evaluate urban sprawl in other metropolises in Ghana or similar developing countries.

Note

1. Details of the concentric zone theory as well as other sprawl theories such as Von Thünen, Central Place, Sector, Multi Nuclei Bid – Rent are presented in Pradhan (2017).

Acknowledgments

My heartfelt gratitude goes to the Federal Ministry of Education and Research (BMBF) and the West African Science Centre on Climate Change and Adapted Land Use (WASCAL) for awarding me the scholarship that supported my PhD research, which led to the creation of this publication

Disclosure statement

No potential conflict of interest was reported by the author(s).

References

Abass, K., Adanu, S. K., & Gyasi, R. M. (2018). Urban sprawl and land use/land-cover transition probabilities in peri-urban Kumasi, Ghana. *West African Journal of Applied Ecology*, *26*, 118–132.

Abass, K., Dumedah, G., Frempong, F., Muntaka, A. S., Appiah, D. O., Garsonu, E. K., & Gyasi, R. M. (2022). Rising incidence and risks of floods in urban Ghana: Is climate change to blame? *Cities*, *121*(September 2021), 103495. https://doi.org/10.1016/j.cities.2021.103495

Abdul-Kareem, R., Gnansounou, S. C., & Adongo, R. (2021). Effects of the oil-find on land management in the Sekondi-Takoradi Metropolis, Western Coast of Ghana. *Journal of Land Use Science*, *16*(4), 398–412. https://doi.org/10.1080/1747423X.2021.1991018

Abdullahi, S., & Pradhan, B. (2010). Urban expansion and change detection analysis. https://doi.org/10.1007/978-3-319-54217-1

Abudu, D., Azo, R., & Andogah, G. (2019). Spatial assessment of urban sprawl in Arua Municipality, Uganda. *The Egyptian Journal of Remote Sensing and Space Sciences*, *22*(3), 315–322. https://doi.org/10.1016/j.ejrs.2018.01.008

Aduah, M. S., & Baffoe, P. E. (2013). Remote sensing for mapping land-use/Cover changes and urban sprawl in Sekondi-Takoradi.

Agenda, D. (2013). *Medium-term national development policy framework : Volume I : Policy framework*. *I*, 2010–2013.

Akubia, J. E. K., & Bruns, A. (2019). Unravelling the frontiers of urban growth: Spatio-Temporal dynamics of land-use change and urban expansion in Greater Accra Metropolitan Area, Ghana. *The Land*, *8*(9), 1–23. https://doi.org/10.3390/land8090131

Al-Hinai, H., & Abdalla, R. (2021). Mapping coastal flood susceptible areas using Shannon's entropy Model: The case of Muscat Governorate, Oman. *ISPRS International Journal of Geo-Information*, *10*(4), 252. https://doi.org/10.3390/ijgi10040252

Alijani, Z., Hosseinali, F., & Biswas, A. (2020). Spatio-temporal evolution of agricultural land use change drivers: A case study from Chalous region, Iran. *Journal of Environmental Management*, *262*(June 2019), 110326. https://doi.org/10.1016/j.jenvman.2020.110326

Alqadhi, S., Mallick, J., Talukdar, S., Bindajam, A. A., & Shohan, A. A. A. (2021). Quantification of urban sprawl for past-to-future in Abha City, Saudi Arabia. *Computer Modeling in Engineering & Sciences*, *129*(2), 755–786. https://doi.org/10.32604/cmes.2021.016640

Alqattan, N., Acheampong, M., Jaward, F. M., Vijayakumar, N., Ebude, L., & Enomah, D. (2019). Evaluation of the potential hydrological impacts of land use/cover change dynamics in Ghana's oil city. *Development and Sustainability*, *22*(8), 7313–7330. https://doi.org/10.1007/s10668-019-00507-0

Annim, A. (2023, October 27). Construction of first-ever interchange in Western Region.

Anwar, M., Asming, A., Ibrahim, A. M., & Abir, I. M. (2022). Processing and classification of landsat and sentinel images for oil palm plantation detection. *Remote Sensing Applications: Society & Environment*, *26*, 100747. https://doi.org/10.1016/j.rsase.2022.100747

Appiah, D. O. (2016). *Geoinformation Modelling of Peri-Urban Land Use and Land Cover Dynamics for Climate Variability and Climate Change in the Bosomtwe District, Ghana*.

Asare, Y. M., Selby, I., Ashiagbor, G., & Asante, C. Y. (2023). Analysis and prediction of land use land cover dynamics in the Kpeshie Lagoon Basin of Ghana using satellite remote sensing. *Journal of the Ghana Institution of Engineering (JghIE)*, *23*(1), 33–43. https://doi.org/10.56049/jghie.v23i1.64

Biney, E., Biney, N., Dadzie, I., Harris, E., Ama, G., Mensah, Y., Bessah, E., & Kwabena, E. (2022). Impact of mining on vegetation cover: A case study of Prestea Huni-Valley municipality. *Scientific African*, *17*, e01387. https://doi.org/10.1016/j.sciaf.2022.e01387

Biney, E., & Boakye, E. (2021). Urban sprawl and its impact on land use land cover dynamics of sekondi-takoradi metropolitan assembly, Ghana. *Environmental Challenges*, *4*(April), 100168. https://doi.org/10.1016/j.envc.2021.100168

Cengiz, S., Gormüs, S., & Oguz, D. (2022). Analysis of the urban growth pattern through spatial metrics ; Ankara City. *Land Use Policy*, *112*(January 2021), 105812. https://doi.org/10.1016/j.landusepol.2021.105812

Chettry, V. (2022). Peri-urban area delineation and urban sprawl quantification in Thiruvananthapuram Urban agglomeration, India, from 2001 to 2021 using geoinformatics. *Applied Geomatics*, *14*(4), 639–652. https://doi.org/10.1007/s12518-022-00460-0

Chong, C. H. (2017). *Comparison of Spatial Data Types for Urban Sprawl Analysis Using Shannon ' S Entropy*.

Daata, E., Kwabena, E., Biney, E., Harris, E., & Quaye-Ballard, J. A. (2021). The impact of land use and land cover changes on socioeconomic factors and livelihood in the Atwima Nwabiagya district of the Ashanti region, Ghana. *Environmental Challenges*, *5*(July), 100226. https://doi.org/10.1016/j.envc.2021.100226

Dadzie-Paintsil, E., & Mensah, J. V. (2022). Effects of urbanization on coastal wetlands in the Sekondi-Takoradi Metropolis, Ghana. *Indo Pacific Journal of Ocean Life*, *6*(2). https://doi.org/10.13057/oceanlife/o060205

Danso, S. Y., & Addo, I. Y. (2018). Coping strategies of households affected by flooding: A case study of sekondi-takoradi metropolis in Ghana. *Urban Water Journal*, *July*, 1–7. https://doi.org/10.1080/1573062X.2016.1176223

Deribew, K. T. (2020). Spatiotemporal analysis of urban growth on forest and agricultural land using geospatial techniques and Shannon entropy method in the satellite town of Ethiopia, the western fringe of Addis Ababa city. *Ecological Processes*, *9*(1). https://doi.org/10.1186/s13717-020-00248-3

Dijkstra, L., Galic, A., & Brandmüller, T. (2022). Measuring sustainable development goals in cities, towns and rural areas: The new degree of Urbanisation1. *Statistical Journal of the IAOS*, *38*(2), 549–559. https://doi.org/10.3233/SJI-220020

Doe, B., Amoako, C., & Adamtey, R. (2022). Spatial expansion and patterns of land use/land cover changes around Accra, Ghana – emerging insights from Awutu Senya East Municipal Area. *Land Use Policy*, *112*(August 2021), 105796. https://doi.org/10.1016/j.landusepol.2021.105796

Feng, Q., & Gauthier, P. (2021). Untangling urban sprawl and climate change: A review of the literature on physical planning and transportation drivers. *Atmosphere*, *12*(5), 547. https://doi.org/10.3390/atmos12050547

Fernández-Delgado, M. (2014). Do we need hundreds of classifiers to solve real world classification problems? *The Journal of Machine Learning Research*, *15*(1), 3133–3181.

Fiave, R. E. (2017). Sekondi-Takoradi as an Oil City. *37*(1), 61–79.

Foody, G. M. (2020). Explaining the unsuitability of the kappa coefficient in the assessment and comparison of the accuracy of thematic maps obtained by image classification. *Remote Sensing of Environment*, *239*, 111630. https://doi.org/10.1016/j.rse.2019.111630

Friedrich, H. K. (2021). Satellite-based human settlement datasets inadequately detect refugee settlements: A critical assessment at thirty refugee settlements in Uganda. 15–17.
Frimpong, K., Eugene, D., & Van Etten, E. J. (2022). Urban sprawl and microclimate in the Ga east municipality of Ghana. *Heliyon*, *8*(7), e09791. https://doi.org/10.1016/j.heliyon.2022.e09791
García-Álvarez, D., Teresa, M., & Olmedo, C. (2022). *Land use cover datasets and validation tools*. Springer International Publishing. https://doi.org/10.1007/978-3-030-90998-7
Gašparović, M. (2020). *Urban growth pattern detection and analysis* (pp. 35–48). https://doi.org/10.1016/B978-0-12-820730-7.00003-3(). (pp. 35.
Getu, K., & Bhat, H. G. (2021). Analysis of spatio-temporal dynamics of urban sprawl and growth pattern using geospatial technologies and landscape metrics in Bahir Dar, Northwest Ethiopia. *Land Use Policy*, *109*(August), 105676. https://doi.org/10.1016/j.landusepol.2021.105676
Ghana Ports and Harbours Authority. (2016) Our History and Future, Takoradi Port. http://www.ghanaports.gov.gh/page/27/Takoradi-Port-Our-History-And-F
Haas, J. (2013). *Remote sensing of urbanization and environmental impacts* (issue June).
Hackman, K. O., Li, X., Asenso-Gyambibi, D., Emmanuella, A., & Nelson, I. D. (2020). Analysis of geo-spatiotemporal data using machine learning algorithms and reliability enhancement for urbanization decision support. *International Journal of Digital Earth*, *13*(12), 1717–1732. https://doi.org/10.1080/17538947.2020.1805036
Hasan, M., Haque, R., & Rahman, M. (2023). Identifying the land use land cover (LULC) changes using remote sensing and GIS approach: A case study at Bhaluka in Mymensingh, Bangladesh. *Case Studies in Chemical and Environmental Engineering*. https://doi.org/10.1016/j.cscee.2022.100293
Hidalgo-García, D., & Arco-Díaz, J. (2022). Modeling the surface urban heat island (SUHI) to study of its relationship with variations in the thermal field and with the indices of land use in the metropolitan area of Granada (Spain). *Sustainable Cities and Society*, *87*, 104166. https://doi.org/10.1016/j.scs.2022.104166
Ibrahim, R. E., Taha, L. G., & Shalaby, A. (2019). Urban expansion and pattern analysis using Shannon's entropy approach in ElMinya. *13*, 637–646.
Kamruzzaman, M., Deilami, K., & Yigitcanlar, T. (2018). Investigating the urban heat island effect of transit oriented development in Brisbane. *Journal of Transport Geography*, *66*, 116–124. https://doi.org/10.1016/j.jtrangeo.2017.11.016
Krishnaveni, K. S., & Anil, P. P. (2022). Spatio-temporal dynamics of urban sprawl in a rapidly urbanizing city using machine learning classification. *Geocarto International*, *37*(27), 17403–17434. https://doi.org/10.1080/10106049.2022.2129817
Larbi, I. (2023). Land use-land cover change in the tano basin, Ghana and the implications on sustainable development goals. *Heliyon*, *9*(4), e14859. https://doi.org/10.1016/j.heliyon.2023.e14859
Manesha, E. P. P., Jayasinghe, A., & Nawod, H. (2021). Measuring urban sprawl of small and medium towns using GIS and remote sensing techniques: A case study of Sri Lanka. *The Egyptian Journal of Remote Sensing and Space Sciences*, *24*(3), 1051–1060. https://doi.org/10.1016/j.ejrs.2021.11.001
Mensah, C. A., Eshun, J. K., Asamoah, Y., & Ofori, E. (2019). Changing land use/cover of Ghana ' s oil city (sekondi-takoradi metropolis): Implications for sustainable urban development. https://doi.org/10.1080/19463138.2019.1615492
Mohammadian, H., Tavakoli, J., & Khani, H. (2017). Monitoring land use change and measuring urban sprawl based on its spatial forms the case of qom city. *The Egyptian Journal of Remote Sensing and Space Sciences*, *20*(1), 103–116. https://doi.org/10.1016/j.ejrs.2016.08.002
Mukherjee, F., & Singh, D. (2020). Assessing land use – land cover change and its impact on land surface temperature using LANDSAT data: A comparison of two urban areas in India. *Earth Systems and Environment*, *4*(2), 385–407. https://doi.org/10.1007/s41748-020-00155-9
Nyamekye, C., Kwofie, S., Ghansah, B., Agyapong, E., & Appiah, L. (2020). Assessing urban growth in Ghana using machine learning and intensity analysis: A case study of the new juaben municipality. *Land Use Policy*, *99*(August), 105057. https://doi.org/10.1016/j.landusepol.2020.105057
Obeng, K., Forkuo, E. K., Asare, Y. M., Opoku, P., & Obeng, A. S. (2023). Land use land cover changes in the Densu River Basin of Ghana from 1991 to 2020. *41*(1), 1–18.
Østby, G. (2016). Rural–urban migration, inequality and urban social disorder: Evidence from African and Asian cities. *Conflict Management and Peace Science*, *33*(5), 491–515. https://doi.org/10.1177/0738894215581315
Pradhan, B. (2017). Spatial modeling and assessment of urban form.
Rainey, J. L., Brody, S. D., Galloway, G. E., & Highfield, W. E. (2021). Assessment of the growing threat of urban flooding: A case study of a national survey. *Urban Water Journal*, 1–7. https://doi.org/10.1080/1573062X.2021.1893356
Rana, S., & Sarkar, S. (2021). Prediction of urban expansion by using land cover change detection approach. *Heliyon*, *7*(August), e08437. https://doi.org/10.1016/j.heliyon.2021.e08437

Saha, S., Saha, A., Das, M., Saha, A., Sarkar, R., & Das, A. (2021). Analyzing spatial relationship between land use/land cover (LULC) and land surface temperature (LST) of three urban agglomerations (UAs) of Eastern India. *Remote Sensing Applications: Society & Environment*, *22*(April), 100507. https://doi.org/10.1016/j.rsase.2021.100507

Service, G. S. (2014). Ghana *2010 population and housing census*.

Service, G. S. (2021). *Ghana 2021 population and housing census*.

Shamsudeen, M., Padmanaban, R., Cabral, P., & Morgado, P. (2022). Spatio-temporal analysis of the impact of landscape changes on vegetation and land surface temperature over Tamil Nadu. *MDPI*, *3*(2), 614–638. https://doi.org/10.3390/earth3020036

Shao, Z., Sumari, N. S., Portnov, A., Ujoh, F., & Mandela, P. J. (2021). Urban sprawl and its impact on sustainable urban development: A combination of remote sensing and social media data. *Geo-Spatial Information Science*, *24*(2), 241–255. https://doi.org/10.1080/10095020.2020.1787800

Shikary, C., & Rudra, S. (2020). Measuring urban land use change and sprawl using geospatial techniques: A study on Purulia Municipality, West Bengal, India. *Journal of the Indian Society of Remote Sensing*, *49*(2), 433–448. https://doi.org/10.1007/s12524-020-01212-6

Stemn, E., & Agyapong, E. (2014). Assessment of urban expansion in the sekondi-takoradi metropolis of Ghana using remote-sensing and GIS approach. *3*(8).

Steurer, M., & Bayr, C. (2020). Measuring urban sprawl using land use data. *Land Use Policy*, *97*(December 2019), 104799. https://doi.org/10.1016/j.landusepol.2020.104799

Sumari, S. N., Cobbinah, B. P., Ujoh, F., & Xu, G. (2020). On the absurdity of rapid urbanization: Spatio-temporal analysis of land-use changes in Morogoro, Tanzania. *Cities*, *107*(July), 102876. https://doi.org/10.1016/j.cities.2020.102876

Surya, B., Salim, A., Hernita, H., Suriana, S., Menne, F., & Rasyidi, S. E. (2021). Land use change, urban agglomeration, and urban sprawl: A sustainable development perspective of Makassar City, Indonesia. *The Land*, *10*(6), 556. https://doi.org/10.3390/land10060556

Tariq, A., Yan, J., & Mumtaz, F. (2022). Land change modeler and CA-Markov chain analysis for land use land cover change using satellite data of Peshawar, Pakistan. *Physics and Chemistry of the Earth*, *128*(October), 103286. https://doi.org/10.1016/j.pce.2022.103286

United Nations. (2015) Sustainable development goals. https://sustainabledevelopment.un.org/

United Nations World Population Prospect. (2023).https://www.macrotrends.net.

Verma, S., Agrawal, S., & Dutta, K. (2021) Satellite imagery driven assessment of land use land cover, urbanization and surface temperature pattern dynamics. November, 17–19.

Vinh, T., & Nguyen, D. (2019). *Transcalar Urban Governance: Planning and Development in the "Oil-City" of Sekondi-Takoradi, Ghana*.

Wangyel, S., Munkhnasan, L., & Lee, W. (2021). Land use and land cover change detection and prediction in Bhutan' s high altitude city of Thimphu, using cellular automata and Markov chain. *Environmental Challenges*, *2*(November 2020), 100017. https://doi.org/10.1016/j.envc.2020.100017

Xiang, X., Qiu, C., Hu, J., Shi, Y., Wang, Y., Schmitt, M., & Taubenb, H. (2022). The urban morphology on our planet – global perspectives from space. *Remote Sensing of Environment*, *269*(September 2021), 1–11. https://doi.org/10.1016/j.rse.2021.112794